ACS Photonics

pubs.acs.org/journal/apchd5

Article

Mie-Driven Ultrafast Faraday Rotation in Magnetophotonic Metasurfaces

Anna M. Chernyak, Alexander I. Musorin, and Andrey A. Fedyanin*

Cite This: *ACS Photonics* 2026, 13, 4799−4805

Read Online

ACCESS | Metrics & More | Article Recommendations | Supporting Information

ABSTRACT: We report ultrafast Faraday rotation dynamics inside a single femtosecond pulse transmitted through a Mie-resonant semiconductor metasurface covered with a thin ferromagnetic film. Time-resolved cross-correlation measurements reveal intrapulse polarization rotation with a relative modulation of 55% over 500 fs at the wavelength of the merged magnetic and electric dipole Mie resonances. These results may be applicable to subpicosecond polarization state control in integrated optical nonreciprocal isolators, ultrafast modulators, sensors, and optical signal processing units.

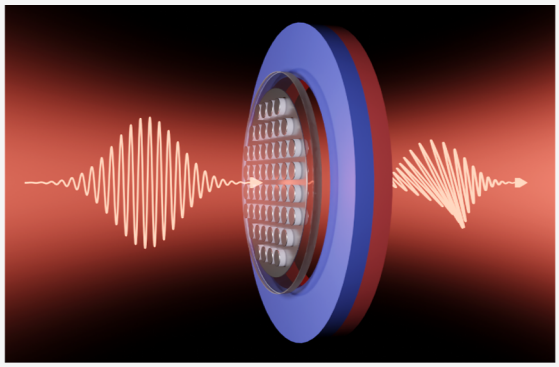

KEYWORDS: *ultrafast processes, magneto-optics, metasurfaces, Faraday effect, Mie resonances*

INTRODUCTION

Dynamic light polarization control is crucial for technologies ranging from liquid-crystal displays and fiber-optic telecommunications to quantum-state preparation and ultrafast polarimetry. Liquid-crystal-based devices offer a wide tunability of polarization state control but suffer from slow operating time. Meanwhile, magneto-optical (MO) cells demonstrate fast operation, but their dimensions are not suitable for compact applications such as integrated photonic circuits. This gap calls for the development of a tiny ultrafast polarization control device.

Magneto-optical effects enable not only the analysis of magnetic properties of samples[1] but also facilitate light polarization or intensity modulation without mechanical motion as well.[2] However, MO response at the optical frequencies is inherently weak, driving the search for ways to enhance it. A promising approach involves integrating magnetic materials with nanostructures that support optical resonances, which can amplify MO effects by several orders of magnitude.[3−13] Recently, silicon nanodisks covered by a thin nickel layer have been introduced for boosting magneto-optical Kerr and Faraday effects.[14−16]

Optical isolators play an essential role in laser experiments, preserving sensitive radiation sources from damage. Their operating principle often relies on the magneto-optical Faraday effect. Analogous to an optical diode, a Faraday rotator transmits linearly polarized light in one direction, rotating its polarization by 45°, while suppressing backward-propagating waves, which become orthogonally polarized due to the nonreciprocity of the Faraday effect. This nonreciprocity requires breaking time-reversal symmetry, which is achieved by applying an external magnetic field. These devices can be understood in terms of topological insulators, as they represent unidirectional propagation channels for light.[17] The search for topological nanophotonic systems opens new strategies for light control applications by breaking reciprocity in miniature devices. Modern nanophotonics leverages high-index, low-absorption particles, usually made of semiconductors.[18] Such nanoobjects exhibit a sensitive response to a light wave caused by scattering resonances.[19,20] Electromagnetic radiation concentrates effectively inside semiconductor particles if its frequency coincides with eigenfrequencies of the nanoparticle. The resonance lifetime and the decay rate are determined by the interaction time between the light and the particle. Such quenching can be expressed as the sum of radiative and nonradiative losses. The latter is negligible for high-index particles at the visible and near-IR spectral ranges. The former depends on the type of eigenmode. Lower-order optical dipole Mie resonances possess relatively low quality factors ($Q \approx 10$) and exhibit broad spectral widths. The lifetime of such resonances corresponds to the femtosecond scale, determining the effective light−matter interaction time. Excitation of high-

Received: May 5, 2026
Revised: July 22, 2026
Accepted: July 22, 2026
Published: July 30, 2026

https://doi.org/10.1021/acsphotonics.6c01095
ACS Photonics 2026, 13, 4799−4805

order Mie modes or packing nanocavities into metasurfaces allows achieving much higher Q-factors with longer lifetimes.[21−23] Strong optical magnetism arising from Mie-type resonances in high-index semiconductor metasurfaces leads to a number of promising phenomena.[24−26]

Femtosecond time-resolved pump−probe spectroscopy is one of the most powerful tools for studying carrier dynamics in solid-state physics,[27−30] realizing ultrafast all-optical switching,[31−33] sensing the magnetic subsystem of the sample,[34−38] and controlling magnetic order.[39−42] Nontrivial behavior of magneto-optical effects is observed in magnetophotonic[43] and magnetoplasmonic[44] crystals when the ultrashort laser pulse duration is comparable to the resonance lifetime. However, there is a lack of research on the intrapulse evolution of polarization rotation caused by Mie resonances on the femtosecond time scale. Recently, ultrafast all-optical polarization switching in Mie-resonance-based hybrid metasurfaces consisting of an array of amorphous silicon nanodisks on a gold backplane was demonstrated, but only numerically.[45] Reflection can be altered dynamically through the photoinduced carriers in α − Si:H, resulting in ultrafast polarization variation. In our paper, we experimentally demonstrate ultrafast modulation of the polarization state. We study peculiarities of ultrafast Faraday rotation dynamics in silicon nanodisks with a 6 nm-thick nickel film on top (Figure 1a) both

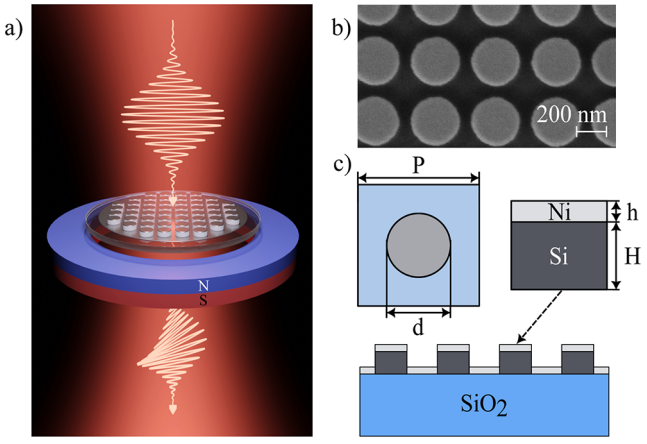

Figure 1. (a) Conceptional representation of ultrafast Faraday rotation by NiSi metasurface. (b) Scanning electron microscopy image of the sample. (c) Schematics of the model with parameters.

experimentally and numerically. We discover a spectrally dependent variation of the time derivative of polarization rotation in the vicinity of Mie resonances. These pilot experiments offer promising prospects for next-generation nonreciprocal modulators based on Mie-resonant nanophotonic elements.

Steady-State Optical and Magneto-Optical Spectroscopy

A magnetophotonic metasurface consisting of a 2D array of silicon nanodisks placed on a SiO_2 substrate and covered with a nickel film is chosen for experimental study of femtosecond Faraday rotation dynamics. The Si disks height H, diameter d, and lattice constant P are selected to overlap the electric and magnetic dipole Mie resonances (ED and MD, respectively) in the vicinity of 800 nm. The parameters are H = 145 nm, d = 310 nm, and P = 400 nm for both in-plane directions (see Figure 1c). An effective nickel layer thickness of h = 6 nm is assumed; the ferromagnetic material coats the silicon disks and fills the gaps between them. Details of the fabrication process can be found in the Supporting Information. Figure 1b shows a scanning electron microscope image of the sample, illustrating the high uniformity and quality of the Si nanodisks. The metasurface has the lateral size of 500 × 500 μm^2.

The largest achievable steady-state Faraday rotation θ in such magnetophotonic metasurfaces occurs when the MD and ED resonances spectrally overlap, as predicted by previous calculations.[46] The desired spectral range to excite this merged ED-MD resonance near the wavelength of 800 nm is dictated by the characteristics of a Ti:sapphire laser, which generates maximal power in this spectral range during the experiment. The steady-state and ultrafast numerical analysis for the case of separated ED and MD resonances is presented in the Supporting Information for comparison, along with mode decomposition. The overlapped ED-MD resonance position of the fabricated metasurface turns out to be at the wavelength of 807 nm, with a transmittance of T = 2.0% (see Figure 2, black

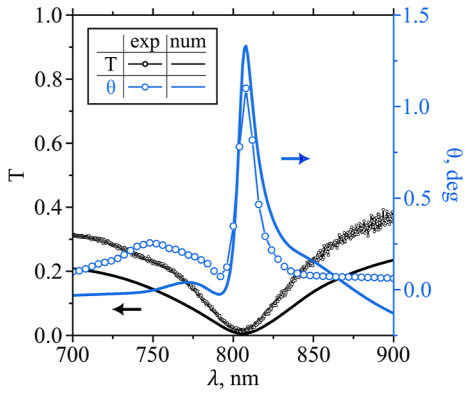

Figure 2. Transmittance (black) and Faraday rotation (blue) spectra of magnetophotonic metasurface with overlapped resonances. Curves are numerical calculations, dots are experiment.

curve with dots). The selected lattice constants leave a diffraction radiation leakage channel below the wavelength λ = 580 nm. The details of the experimental setup for transmittance measurements are described in the Supporting Information. The experimental data (black and blue dots) agree well with the numerical results (black and blue curves). The optical constants of silicon and nickel are taken from the literature.[47,48] The refractive index of the quartz substrate is assumed to be nondispersive and fixed at n = 1.45 in the calculations. The discrepancies in absolute values can be explained by variation in the material dispersion parameters between the real sample and the model (e.g., higher absorption values in the simulations).

The steady-state Faraday rotation spectrum is measured with a polarization-sensitive setup based on a photoelastic modulator (PEM). The polarization plane rotation is proportional to the ratio of the AC (at the PEM's double frequency) and DC components of the photocurrent.[49] The experimental scheme details with a typical spectrum of a laser pulse are given in the Supporting Information. The measured polarization rotation spectrum is shown in Figure 2 by blue dots. The Faraday rotation reaches its maximal value of θ = 1.1° at the resonant wavelength. An unstructured nickel film of the same thickness yields the Faraday rotation of only θ = 0.04° in this spectral region, which is 2 orders of magnitude smaller than the Mie-resonance-enhanced value observed in the metasurface

https://doi.org/10.1021/acsphotonics.6c01095
ACS Photonics 2026, 13, 4799−4805

(see Supporting Information for details). The results are in good agreement with the numerical simulation data (see Figure 2, blue curve). The deviations can be explained by slight variation in the Si disks diameter over the spot area.

Subpicosecond Dynamics of Faraday Effect

Ultrafast MO dynamics is measured using a cross-correlation scheme. Full description of the time-resolved experiment can be found in the Supporting Information. Briefly, the intensity of the light transmitted through the sample and PEM-based polarization-sensitive part of the optical setup (signal pulse) is given by $I_s(t)[1+4J_2(A_0)\theta(t)\cos(4\pi fT)]$, where $\theta(t)$ corresponds to the time-dependent Faraday rotation angle and other quantities are explained in the Supporting Information. The cross-correlation function $u(\tau)$ can be represented as

$$u(\tau) = [1 + 4J_2(A_0)\theta(\tau)\cos(4\pi fT)] \underbrace{\int_{-\infty}^{\infty} I_s(t)I_r(t-\tau)dt}_{u_{DC}}$$

$$= u_{DC}(\tau) + u_{AC}(\tau)\cos(4\pi fT)$$

where $u_{AC}(\tau) = 4J_2(A_0)\theta(\tau)u_{DC}(\tau)$, and $I_r(t-\tau)$ is a reference laser pulse passed through a delay line. The polarization rotation $\theta(\tau)$ is now determined by the ratio of Fourier amplitudes at the PEM's $2f$ frequency u_{AC} and DC u_{DC}

$$\theta(\tau) = \frac{u_{AC}(\tau)}{4J_2(A_0)u_{DC}(\tau)}$$

The normalized cross-correlation function of the pulse transmitted through the sample has a full-width at half-maximum of 260 fs and is shown by the shaded area for the resonant wavelength in Figure 3a. The absence of a chirp is verified using GRENOUILLE. It has a similar shape for the other wavelengths as well, but its non-normalized magnitude varies.

The time-resolved measurements are carried out for several wavelengths across the resonance (see Figure 3b).

The brightest effect of the intrapulse Faraday rotation modulation is observed at the resonant wavelength of λ = 807 nm (Figure 3a). The polarization plane angle decreases monotonically from θ_{cc} = 1.38° on the leading edge to θ_{cc} = 0.77° on the trailing edge (Figure 3a, green). The relative modulation of the polarization plane rotation during 500 fs can be evaluated as the difference between these angles divided by the static value: (1.38° − 0.77°)/1.1° = 0.55. The difference between the angles will hereafter be referred to as the magnitude of the dynamics $\Delta\theta_{cc}$; in this case $\Delta\theta_{cc}$ = −0.61°. It should be noted that all these changes occur within a single pulse: at different moments in time, the electric field of the transmitted pulse is oriented in different directions, as shown schematically in Figure 1a. A small shift of the pulse carrier wavelength away from λ = 807 nm leads to suppression of the intrapulse dynamics magnitude $\Delta\theta_{cc}$ (see Figure 3a). The values are $\Delta\theta_{cc}$ = −0.163° for λ = 805 nm (Figure 3a, blue), $\Delta\theta_{cc}$ = −0.6° for λ = 810 nm (Figure 3a, orange), and $\Delta\theta_{cc}$ = −0.143° for λ = 813 nm (Figure 3a, red). The absolute values of time-dependent Faraday rotation θ_{cc} for the wavelength of λ = 810 nm slightly exceed those for the resonant wavelength of λ = 807 nm but yield a lower dynamics magnitude $\Delta\theta_{cc}$. This may be due to a slight misalignment in the experimental setup, sample imperfections or instability of the pulse generation, leading to small variations in the emitted wavelength. Positive dynamics magnitude $\Delta\theta_{cc}$ = +0.34° is observed upon further spectral tuning to λ = 800 nm.

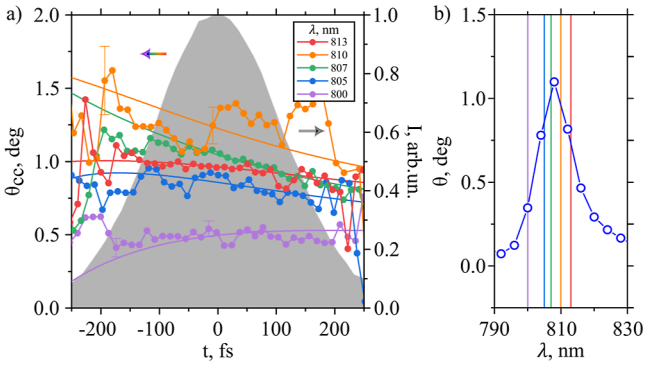

Figure 3. (a) Time-resolved Faraday rotation dynamics. Dots correspond to the experiment, curves are the postprocessed numerical calculations. Colors denote wavelengths: violet is 800 nm, blue is 805 nm, green is 807 nm, orange is 810 nm, red is 813 nm. Shaded area is the cross-correlation function of the pulse. (b) Static experimental Faraday rotation spectrum in vicinity of the mode. Color lines mark the positions of the wavelengths chosen for ultrafast measurements presented in the panel (a).

The color curves in Figure 3a represent results of numerical simulation. Details of the modeling are given in the Supporting Information. Notably, the experimental time dependence is the cross-correlated Faraday rotation, which is not the raw polarization plane rotation angle. The numerical cross-correlated Faraday rotation dynamics is retrieved from the calculated time-dependent veritable Faraday rotation $\theta(t)$, the intensities of the incoming $I_i(t)$ and the transmitted $I_{tr}(t)$ pulses according to the equation

$$\theta_{cc}(t) = \frac{\int \theta(\tau)I_{tr}(\tau)I_i(t-\tau)d\tau}{\int I_{tr}(\tau)I_i(t-\tau)d\tau} \quad (1)$$

where τ is the delay time between the signal (transmitted) and gate (incoming) pulses. This procedure reproduces the polarization angle measurement by the experimental setup (see Supporting Information for details). The obtained experimental and numerical results are in good agreement within the error bars. The difference can be attributed to the inherent cross-correlation averaging of the Faraday rotation absolute values and to sample fabrication imperfections.

Meanwhile, Figure 4 shows the raw calculated time-resolved Faraday rotation, which demonstrates much higher values, up to 6° for the resonant wavelength. The shaded gray area represents the electric field modulus of the transmitted pulse at the resonant wavelength of 807 nm normalized to the incoming pulse amplitude. The pulse leading edge exhibits a sharp leap of the polarization plane rotation up to 6° and a smooth decrease with time down to 0.76° (see green curve in Figure 4a). This indicates that the instantaneous value of Faraday rotation can significantly exceed the static or cross-correlated value. Detuning the wavelength by 2 nm from 807 nm in any direction changes the maximum achievable polarization angle from 6° to about 2° but retains the behavior −an initial increase followed by a monotonic decrease (see the blue curve for the wavelength of 805 nm and the yellow curve for the λ = 809 nm in Figure 4a). The main reason for this behavior is the different delay times of the magnetically induced electric field component E_x compared with the original E_y. This magnetically induced component is reradiated

https://doi.org/10.1021/acsphotonics.6c01095
ACS Photonics 2026, 13, 4799−4805

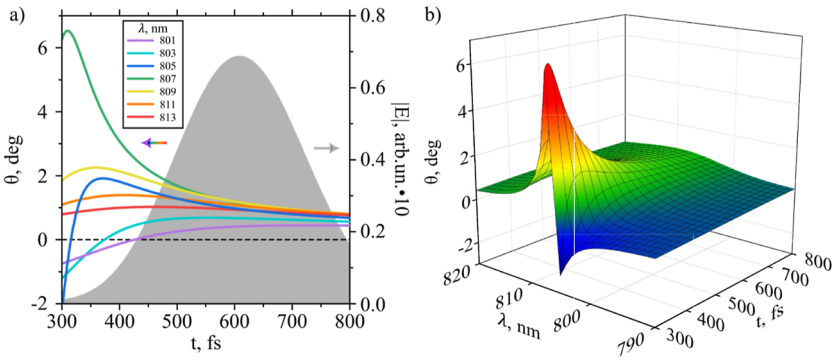

Figure 4. Numerical calculations. (a) Faraday rotation time dependencies for several wavelengths of the pulse for the case of the sample with merged MD-ED resonance. The colors denote various pulse carrier wavelengths: 801 nm (violet), 803 nm (cyan), 805 nm (blue), 807 nm (green), 809 nm (yellow), 811 nm (orange), 813 nm (red). Dashed horizontal lines mark zero Faraday rotation. Shaded area is the transmitted pulse field amplitude. (b) Time-resolved Faraday rotation for wide spectral range in vicinity of the resonances.

earlier, while the original wave still interacts with a nanoresonator (see Supporting Information for details). Further detuning from 807 nm makes the time-resolved Faraday rotation dependence smoother (see the orange, red, cyan and violet curves for λ = 811, 813, 803, and 801 nm, respectively, in Figure 4a). The farther the wavelength is from the resonance, the smoother the temporal magneto-optical dependence becomes (see Figure 4b). An intriguing feature is the zero crossing on the presented time scale for the wavelengths of 801, 803, and 805 nm (violet, cyan, and blue curves in Figure 4a). This means that the polarization at the front of the pulse is rotated in negative direction, while at some moment the electric field is aligned with the incoming radiation (θ = 0°), and the remaining part of the pulse exhibits a polarization rotation that increases with time in the opposite, positive direction. This fact agrees with the experimental cross-correlated data for the wavelength of 800 nm (see Figure 3a, violet). All discussed features of subpicosecond Faraday rotation dynamics are caused by the near-field distribution in the nanoparticles at the merged ED-MD resonance and by the interference of the incoming radiation with the reradiated and delayed light from the Mie-resonant nanodisks covered by the magnetic material.

DISCUSSION

The key finding of this study lies in revealing the nontrivial behavior of the Faraday rotation within a single femtosecond pulse, in contrast to the stationary case for light passing through Mie-resonant magnetophotonic metasurfaces. In the continuous-wave regime, which can be thought of as pulses with an infinitely long duration (much greater than the resonance lifetime), the entire pulse will have the same angle of polarization rotation. Time-resolved studies on specially designed metasurfaces reveal internal nonmonotonic, resonance-induced peculiarities of polarization rotation dynamics.

The experimentally measured static Faraday rotation of θ = 1.1° is consistent with the resonant enhancement levels observed in other nanostructured media. Crucially, our work demonstrates that such measurable effects can be achieved using an ultrathin magnetic layer − merely 6 nm-thick − integrated into the metasurface. In contrast, it has been numerically shown that metasurfaces based on thick bismuth-substituted yttrium iron garnet films (260 nm) achieve larger rotations (e.g., 7.5°[50]) and near-unity transmittance, yielding a high figure of merit (FOM = $|\theta|\sqrt{T}$). However, these advantages come at the cost of significant magnetic material thickness and challenges in garnet nanostructuring.

While the modest transmittance of the structures may seem restrictive, its synergy with the high value of the Faraday effect becomes relevant for specific applications. In systems with back-reflection-sensitive light sources (e.g., distributed feedback lasers, quantum dot lasers), even a small Faraday rotation can be sufficient to suppress feedback in combination with a polarizer. In chips for quantum computing, signal processing, or sensing, isolation of individual components is often required. The studied metasurface, being ultrathin, is ideal for integration. The low transmittance can be compensated for by on-chip amplification, or it is acceptable for short signal transmission distances within a circuit −where operational stability, rather than signal power, is critical. The structure can be used as a compact, magnetic-field-driven polarization modulator in systems where the available baseline intensity is high or the detectors are sufficiently sensitive (e.g., CCD/CMOS cameras, single-photon detectors).

At present, in addition to MO effects such as the Faraday effect, there are other mechanisms that change polarization states in time. In photonic structures based on liquid crystals, the switching time between polarization states is determined by the applied field, lying in the range from microseconds to nanoseconds, which makes them inapplicable for ultrafast applications.[51,52] Pockels cells provide polarization modulation at gigahertz frequencies with picosecond response.[53] However, they require high control voltages and have limited optical stability at high radiation intensities. Plasmonic nanostructures exhibit ultrafast local field dynamics (tens of femtoseconds), but their application is limited by high optical losses due to energy dissipation in the metal.[44] One of the most studied structures for controlling the polarization of light is photonic crystals.[54] Structures with strong dispersion allow slowing down the group velocity of light.[43] If a substance possesses gyrotropy, the efficiency of rotation of the polarization plane per unit length increases sharply. In this case, the rotation itself develops in time as the pulse passes through the slowing structure, which leads to a specific time dependence of the polarization state of the output pulse. However, photonic crystals are strongly inferior to metasurfaces due to their thickness of the structure, which results in a small rotation of the polarization plane per unit length.

A possible application area for the studied nonreciprocal nanophotonic devices is ultrafast polarization modulation

https://doi.org/10.1021/acsphotonics.6c01095
ACS Photonics 2026, 13, 4799−4805

experiments. Recently, a metasurface-based magneto-optical polarization splitter is introduced to split a single femtosecond pulse into two replicas with twice shorter durations and orthogonal polarizations.[16] Similar magnetic metasurfaces under femtosecond pump can generate acoustic excitations[55] or spin waves.[56] Throughout this study we demonstrate the fundamental possibility of creating such structures and provide experimental proof of this technique. To boost the efficiency to applicable values, the static and dynamic values of Faraday rotation should be increased.

CONCLUSION

We experimentally and numerically show peculiarities of subpicosecond Faraday rotation dynamics in magnetophotonic metasurfaces. We discover a spectrally dependent variation of the time derivative of polarization rotation at the merged ED-MD resonance. The relative modulation of the Faraday rotation reaches 55% over 500 fs. These proof-of-principle experiments open the way for nonreciprocal magneto-optical devices based on Mie-resonant nanophotonic elements.

ASSOCIATED CONTENT

Supporting Information

The Supporting Information is available free of charge at https://pubs.acs.org/doi/10.1021/acsphotonics.6c01095.

S1. Sample fabrication details. S2. Numerical calculation method including steady-state and ultrafast Faraday rotation analysis for separated ED and MD resonances, unstructured nickel film analysis, multipole decomposition and dynamics of magnetically induced and original components of electric field transmitted through the metasurface. S3. Experimental setups for transmittance, static Faraday rotation, and femtosecond dynamics measurements (PDF)

AUTHOR INFORMATION

Corresponding Author

Andrey A. Fedyanin − *Faculty of Physics, Lomonosov Moscow State University, 119991 Moscow, Russia;* orcid.org/0000-0003-4708-6895; Email: fedyanin@nanolab.phys.msu.ru

Authors

Anna M. Chernyak − *Department of Materials Science, Shenzhen MSU-BIT University, 517182 Shenzhen, P.R.C; Faculty of Physics, Lomonosov Moscow State University, 119991 Moscow, Russia*

Alexander I. Musorin − *Department of Materials Science, Shenzhen MSU-BIT University, 517182 Shenzhen, P.R.C; Faculty of Physics, Lomonosov Moscow State University, 119991 Moscow, Russia*

Complete contact information is available at: https://pubs.acs.org/10.1021/acsphotonics.6c01095

Funding

Russian Science Foundation (grant No. 25-22-00825); Shenzhen Municipal Government and Shenzhen MSU-BIT University; Foundation for the Advancement of Theoretical Physics and Mathematics "BASIS" for the scholarship award.

Notes

The authors declare no competing financial interest.

ACKNOWLEDGMENTS

The work was performed under financial support of Russian Science Foundation (grant No. 25-22-00825). The reported study was funded by Shenzhen Municipal Government and Shenzhen MSU-BIT University. A.M. Chernyak acknowledges the Foundation for the Advancement of Theoretical Physics and Mathematics "BASIS" for the scholarship award. The work was carried out using the equipment purchased partly by Moscow State University Development Program. The authors thank Dr. D.A. Shilkin.

REFERENCES

(1) Kirilyuk, A.; Kimel, A. V.; Rasing, T. Ultrafast optical manipulation of magnetic order. *Rev. Mod. Phys.* **2010**, *82*, 2731.

(2) Kimel, A.; Zvezdin, A.; Sharma, S.; Shallcross, S.; De Sousa, N.; García-Martín, A.; Salvan, G.; Hamrle, J.; Stejskal, O.; McCord, J.; et al. The 2022 magneto-optics roadmap. *J. Phys. D* **2022**, *55*, 463003.

(3) Martín-Becerra, D.; González-Díaz, J. B.; Temnov, V. V.; Cebollada, A.; Armelles, G.; Thomay, T.; Leitenstorfer, A.; Bratschitsch, R.; García-Martín, A.; González, M. U. Enhancement of the magnetic modulation of surface plasmon polaritons in Au/Co/Au films. *Appl. Phys. Lett.* **2010**, *97*, 183114.

(4) Grunin, A. A.; Zhdanov, A. G.; Ezhov, A. A.; Ganshina, E. A.; Fedyanin, A. A. Surface-plasmon-induced enhancement of magneto-optical Kerr effect in all-nickel subwavelength nanogratings. *Appl. Phys. Lett.* **2010**, *97*, 261908.

(5) Chin, J. Y.; Steinle, T.; Wehlus, T.; Dregely, D.; Weiss, T.; Belotelov, V. I.; Stritzker, B.; Giessen, H. Nonreciprocal plasmonics enables giant enhancement of thin-film Faraday rotation. *Nat. Commun.* **2013**, *4*, 1599.

(6) Banthí, J. C.; Meneses-Rodríguez, D.; García, F.; González, M. U.; García-Martín, A.; Cebollada, A.; Armelles, G. High magneto-optical activity and low optical losses in metal-dielectric Au/Co/Au-SiO_2 magnetoplasmonic nanodisks. *Adv. Mater.* **2012**, *24*..

(7) Bonanni, V.; Bonetti, S.; Pakizeh, T.; Pirzadeh, Z.; Chen, J.; Nogués, J.; Vavassori, P.; Hillenbrand, R.; Åkerman, J.; Dmitriev, A. Designer magnetoplasmonics with nickel nanoferromagnets. *Nano Lett.* **2011**, *11*, 5333−5338.

(8) Maccaferri, N.; Inchausti, X.; García-Martín, A.; Cuevas, J. C.; Tripathy, D.; Adeyeye, A. O.; Vavassori, P. Resonant enhancement of magneto-optical activity induced by surface plasmon polariton modes coupling in 2D magnetoplasmonic crystals. *ACS Photonics* **2015**, *2*, 1769−1779.

(9) Kataja, M.; Hakala, T. K.; Julku, A.; Huttunen, M. J.; van Dijken, S.; Törmä, P. Surface lattice resonances and magneto-optical response in magnetic nanoparticle arrays. *Nature Commun.* **2015**, *6*, 7072.

(10) Musorin, A. I.; Chetvertukhin, A. V.; Dolgova, T. V.; Uchida, H.; Inoue, M.; Luk'Yanchuk, B. S.; Fedyanin, A. A. Tunable multimodal magnetoplasmonic metasurfaces. *Appl. Phys. Lett.* **2019**, *115*, 151102.

(11) Ignatyeva, D. O.; Karki, D.; Voronov, A. A.; Kozhaev, M. A.; Krichevsky, D. M.; Chernov, A. I.; Levy, M.; Belotelov, V. I. All-dielectric magnetic metasurface for advanced light control in dual polarizations combined with high-Q resonances. *Nature Commun.* **2020**, *11*, 5487.

(12) López-Ortega, A.; Zapata-Herrera, M.; Maccaferri, N.; Pancaldi, M.; Garcia, M.; Chuvilin, A.; Vavassori, P. Enhanced magnetic modulation of light polarization exploiting hybridization with multipolar dark plasmons in magnetoplasmonic nanocavities. *Light: Sci. Appl.* **2020**, *9*, 49.

(13) Makarova, A. V.; Nerovnaya, A. A.; Gulkin, D. N.; Popov, V. V.; Frolov, A. Y.; Fedyanin, A. A. Goos−Hänchen Shift Spatially Resolves Magneto-Optical Kerr Effect Enhancement in Magnetoplasmonic Crystals. *ACS Photonics* **2024**, *11*, 1619−1626.

(14) Barsukova, M. G.; Shorokhov, A. S.; Musorin, A. I.; Neshev, D. N.; Kivshar, Y. S.; Fedyanin, A. A. Magneto-optical response enhanced by Mie resonances in nanoantennas. *ACS Photonics* **2017**, *4*, 2390−2395.
(15) Barsukova, M. G.; Musorin, A. I.; Shorokhov, A. S.; Fedyanin, A. A. Enhanced magneto-optical effects in hybrid Ni-Si metasurfaces. *APL Photonics* **2019**, *4*, 016102.
(16) Chernyak, A. M.; Musorin, A. I.; Fedyanin, A. A. Faraday Rotation Dynamics in Hybrid Magnetophotonic Metasurfaces. *Moscow Univ. Phys. Bull.* **2024**, *79*, 592−595.
(17) Haldane, F. D. M.; Raghu, S. Possible realization of directional optical waveguides in photonic crystals with broken time-reversal symmetry. *Phys. Rev. Lett.* **2008**, *100*, 013904.
(18) Kuznetsov, A. I.; Miroshnichenko, A. E.; Brongersma, M. L.; Kivshar, Y. S.; Luk'yanchuk, B. Optically resonant dielectric nanostructures. *Science* **2016**, *354*, aag2472.
(19) Bohren, C. F.; Huffman, D. R. *Absorption and Scattering of Light by Small Particles*; A Wiley-Interscience Publication, 1998.
(20) Evlyukhin, A. B.; Novikov, S. M.; Zywietz, U.; Eriksen, R. L.; Reinhardt, C.; Bozhevolnyi, S. I.; Chichkov, B. N. Demonstration of magnetic dipole resonances of dielectric nanospheres in the visible region. *Nano Lett.* **2012**, *12*, 3749−3755.
(21) Decker, M.; Staude, I.; Falkner, M.; Dominguez, J.; Neshev, D. N.; Brener, I.; Pertsch, T.; Kivshar, Y. S. High-efficiency dielectric Huygens' surfaces. *Adv. Opt. Mater.* **2015**, *3*, 813−820.
(22) Koshelev, K.; Lepeshov, S.; Liu, M.; Bogdanov, A.; Kivshar, Y. Asymmetric metasurfaces with high-Q resonances governed by bound states in the continuum. *Phys. Rev. Lett.* **2018**, *121*, 193903.
(23) Chernyak, A. M.; Barsukova, M. G.; Shorokhov, A. S.; Musorin, A. I.; Fedyanin, A. A. Bound states in the continuum in magnetophotonic metasurfaces. *JETP Lett.* **2020**, *111*, 46−49.
(24) Della Valle, G.; Hopkins, B.; Ganzer, L.; Stoll, T.; Rahmani, M.; Longhi, S.; Kivshar, Y. S.; De Angelis, C.; Neshev, D. N.; Cerullo, G. Nonlinear Anisotropic Dielectric Metasurfaces for Ultrafast Nanophotonics. *ACS Photonics* **2017**, *4*, 2129−2136.
(25) Shilkin, D. A.; Shcherbakov, M. R.; Lyubin, E. V.; Katamadze, K. G.; Kudryavtsev, O. S.; Sedov, V. S.; Vlasov, I. I.; Fedyanin, A. A. Optical magnetism and fundamental modes of nanodiamonds. *ACS Photonics* **2017**, *4*, 1153−1158.
(26) Mamian, K. A.; Popov, V. V.; Frolov, A. Y.; Fedyanin, A. A. Tailoring transverse magneto-optical Kerr effect enhancement in Mie-resonant nanowire-based metasurfaces. *Appl. Phys. Lett.* **2025**, *126*, 081701.
(27) Schoenlein, R. W.; Lin, W. Z.; Fujimoto, J. G.; Eesley, G. L. Femtosecond studies of nonequilibrium electronic processes in metals. *Phys. Rev. Lett.* **1987**, *58*, 1680.
(28) Ulbricht, R.; Hendry, E.; Shan, J.; Heinz, T. F.; Bonn, M. Carrier dynamics in semiconductors studied with time-resolved terahertz spectroscopy. *Rev. Mod. Phys.* **2011**, *83*, 543.
(29) Johannsen, J. C.; Ulstrup, S.; Cilento, F.; Crepaldi, A.; Zacchigna, M.; Cacho, C.; Turcu, I. C. E.; Springate, E.; Fromm, F.; Raidel, C.; et al. Direct view of hot carrier dynamics in graphene. *Phys. Rev. Lett.* **2013**, *111*, 027403.
(30) Narang, P.; Sundararaman, R.; Atwater, H. A. Plasmonic hot carrier dynamics in solid-state and chemical systems for energy conversion. *Nanophotonics* **2016**, *5*, 96−111.
(31) Mazurenko, D. A.; Kerst, R.; Dijkhuis, J. I.; Akimov, A. V.; Golubev, V. G.; Kurdyukov, D. A.; Pevtsov, A. B.; Sel'Kin, A. V. Ultrafast optical switching in three-dimensional photonic crystals. *Phys. Rev. Lett.* **2003**, *91*, 213903.
(32) Shcherbakov, M. R.; Vabishchevich, P. P.; Shorokhov, A. S.; Chong, K. E.; Choi, D.-Y.; Staude, I.; Miroshnichenko, A. E.; Neshev, D. N.; Fedyanin, A. A.; Kivshar, Y. S. Ultrafast all-optical switching with magnetic resonances in nonlinear dielectric nanostructures. *Nano Lett.* **2015**, *15*, 6985−6990.
(33) Chai, Z.; Hu, X.; Wang, F.; Niu, X.; Xie, J.; Gong, Q. Ultrafast all-optical switching. *Adv. Opt. Mater.* **2017**, *5*, 1600665.
(34) Davies, C. S.; Bonfiglio, G.; Rode, K.; Besbas, J.; Banerjee, C.; Stamenov, P.; Coey, J. M. D.; Kimel, A. V.; Kirilyuk, A. Exchange-driven all-optical magnetic switching in compensated 3 d ferrimagnets. *Phys. Rev. Res.* **2020**, *2*, 032044.
(35) Novikov, I. A.; Kiryanov, M. A.; Nurgalieva, P. K.; Frolov, A. Y.; Popov, V. V.; Dolgova, T. V.; Fedyanin, A. A. Ultrafast magneto-optics in nickel magnetoplasmonic crystals. *Nano Lett.* **2020**, *20*, 8615−8619.
(36) Mishra, K.; Ciuciulkaite, A.; Zapata-Herrera, M.; Vavassori, P.; Kapaklis, V.; Rasing, T.; Dmitriev, A.; Kimel, A.; Kirilyuk, A. Ultrafast demagnetization in a ferrimagnet under electromagnetic field funneling. *Nanoscale* **2021**, *13*, 19367−19375.
(37) Ghita, A.; Mocioi, T.-G.; Lomonosov, A. M.; Kim, J.; Kovalenko, O.; Vavassori, P.; Temnov, V. V. Anatomy of ultrafast quantitative magnetoacoustics in freestanding nickel thin films. *Phys. Rev. B* **2023**, *107*, 134419.
(38) Mishra, K.; Blank, T. G. H.; Davies, C. S.; Avilés-Félix, L.; Salomoni, D.; Buda-Prejbeanu, L. D.; Sousa, R. C.; Prejbeanu, I. L.; Koopmans, B.; Rasing, T.; et al. Dynamics of all-optical single-shot switching of magnetization in Tb/Co multilayers. *Phys. Rev. Res.* **2023**, *5*, 023163.
(39) Ostler, T. A.; Barker, J.; Evans, R. F. L.; Chantrell, R. W.; Atxitia, U.; Chubykalo-Fesenko, O.; El Moussaoui, S.; Le Guyader, L. B. P. J.; Mengotti, E.; Heyderman, L. J.; et al. Ultrafast heating as a sufficient stimulus for magnetization reversal in a ferrimagnet. *Nature Commun.* **2012**, *3*, 666.
(40) Kataja, M.; Freire-Fernández, F.; Witteveen, J. P.; Hakala, T. K.; Törmä, P.; Van Dijken, S. Plasmon-induced demagnetization and magnetic switching in nickel nanoparticle arrays. *Appl. Phys. Lett.* **2018**, *112*, 072406.
(41) Li, G.; Medapalli, R.; Mentink, J. H.; Mikhaylovskiy, R. V.; Blank, T. G. H.; Patel, S. K. K.; Zvezdin, A. K.; Rasing, T.; Fullerton, E. E.; Kimel, A. V. Ultrafast kinetics of the antiferromagnetic-ferromagnetic phase transition in FeRh. *Nature Commun.* **2022**, *13*, 2998.
(42) Gerevenkov, P. I.; Filatov, I. A.; Kalashnikova, A. M.; Khokhlov, N. E. Unidirectional propagation of spin waves excited by femtosecond laser pulses in a planar waveguide. *Phys. Rev. Appl.* **2023**, *19*, 024062.
(43) Musorin, A. I.; Sharipova, M. I.; Dolgova, T. V.; Inoue, M.; Fedyanin, A. A. Ultrafast Faraday rotation of slow light. *Phys. Rev. Appl.* **2016**, *6*, 024012.
(44) Shcherbakov, M. R.; Vabishchevich, P. P.; Frolov, A. Y.; Dolgova, T. V.; Fedyanin, A. A. Femtosecond intrapulse evolution of the magneto-optic Kerr effect in magnetoplasmonic crystals. *Phys. Rev. B* **2014**, *90*, 201405.
(45) Wu, Y.; Kang, L.; Bao, H.; Werner, D. H. Exploiting Topological Properties of Mie-Resonance-Based Hybrid Metasurfaces for Ultrafast Switching of Light Polarization. *ACS Photonics* **2020**, *7*, 2362−2373.
(46) Musorin, A. I.; Barsukova, M. G.; Shorokhov, A. S.; Luk'yanchuk, B. S.; Fedyanin, A. A. Manipulating the light intensity by magnetophotonic metasurfaces. *J. Magn. Magn. Mater.* **2018**, *459*, 165−170.
(47) Rakić, A. D.; Djurišić, A. B.; Elazar, J. M.; Majewski, M. L. Optical properties of metallic films for vertical-cavity optoelectronic devices. *Appl. Opt.* **1998**, *37*, 5271−5283.
(48) Palik, E. D. *Handbook of Optical Constants of Solids*; Academic Press, 1998.
(49) Hipps, K. W.; Crosby, G. A. Applications of the photoelastic modulator to polarization spectroscopy. *J. Phys. Chem.* **1979**, *83*, 555−562.
(50) Christofi, A.; Kawaguchi, Y.; Alù, A.; Khanikaev, A. B. Giant enhancement of Faraday rotation due to electromagnetically induced transparency in all-dielectric magneto-optical metasurfaces. *Opt. Lett.* **2018**, *43*, 1838−1841.
(51) Ikeda, T.; Tsutsumi, O. Optical switching and image storage by means of azobenzene liquid-crystal films. *Science* **1995**, *268*, 1873−1875.

https://doi.org/10.1021/acsphotonics.6c01095
ACS Photonics 2026, 13, 4799−4805

(52) Geis, M. W.; Lyszczarz, T. M.; Osgood, R. M.; Kimball, B. R. 30 to 50 ns liquid-crystal optical switches. *Opt. Express* **2010**, *18*, 18886−18893.
(53) Bishop, A. I.; Barker, P. F. Subnanosecond Pockels cell switching using avalanche transistors. *Rev. Sci. Instrum.* **2006**, *77*, 044701.
(54) Inoue, M.; Fujikawa, R.; Baryshev, A.; Khanikaev, A.; Lim, P.; Uchida, H.; Aktsipetrov, O.; Fedyanin, A.; Murzina, T.; Granovsky, A. Magnetophotonic crystals. *J. Phys. D* **2006**, *39*, R151.
(55) Alekhin, A.; Lomonosov, A. M.; Leo, N.; Ludwig, M.; Vlasov, V. S.; Kotov, L.; Leitenstorfer, A.; Gaal, P.; Vavassori, P.; Temnov, V. Quantitative ultrafast magnetoacoustics at magnetic metasurfaces. *Nano Lett.* **2023**, *23*, 9295−9302.
(56) Chang, C. L.; Tamming, R. R.; Broomhall, T. J.; Janusonis, J.; Fry, P. W.; Tobey, R. I.; Hayward, T. J. Selective excitation of localized spin-wave modes by optically pumped surface acoustic waves. *Phys. Rev. Appl.* **2018**, *10*, 034068.

https://doi.org/10.1021/acsphotonics.6c01095
ACS Photonics 2026, 13, 4799−4805